Figure S1 presents the NMVOC emission inventories obtained by assimilating TROPOMI satellite observations, while Figure S2 shows the NMVOC emission inventories derived from the combined data of TROPOMI and OMPS satellite observations. The data in Figure S2 represent the average of TROPOMI and OMPS observations, and the uncertainty of the combined data is defined as:

$$\sigma_{\mathrm{COMBINE}} = \frac{\sqrt{\sigma^2_{\mathrm{TROPOMI}} + \sigma^2_{\mathrm{OMPS}}}}{2} \tag{S1}$$

Figure S3 shows the increments in annual emissions obtained from the assimilation of the two datasets. The three top-down emission inventories produced in this study are available on Zenodo. (https://doi.org/10.5281/zenodo.14633919; Canjie Xu, 2025).

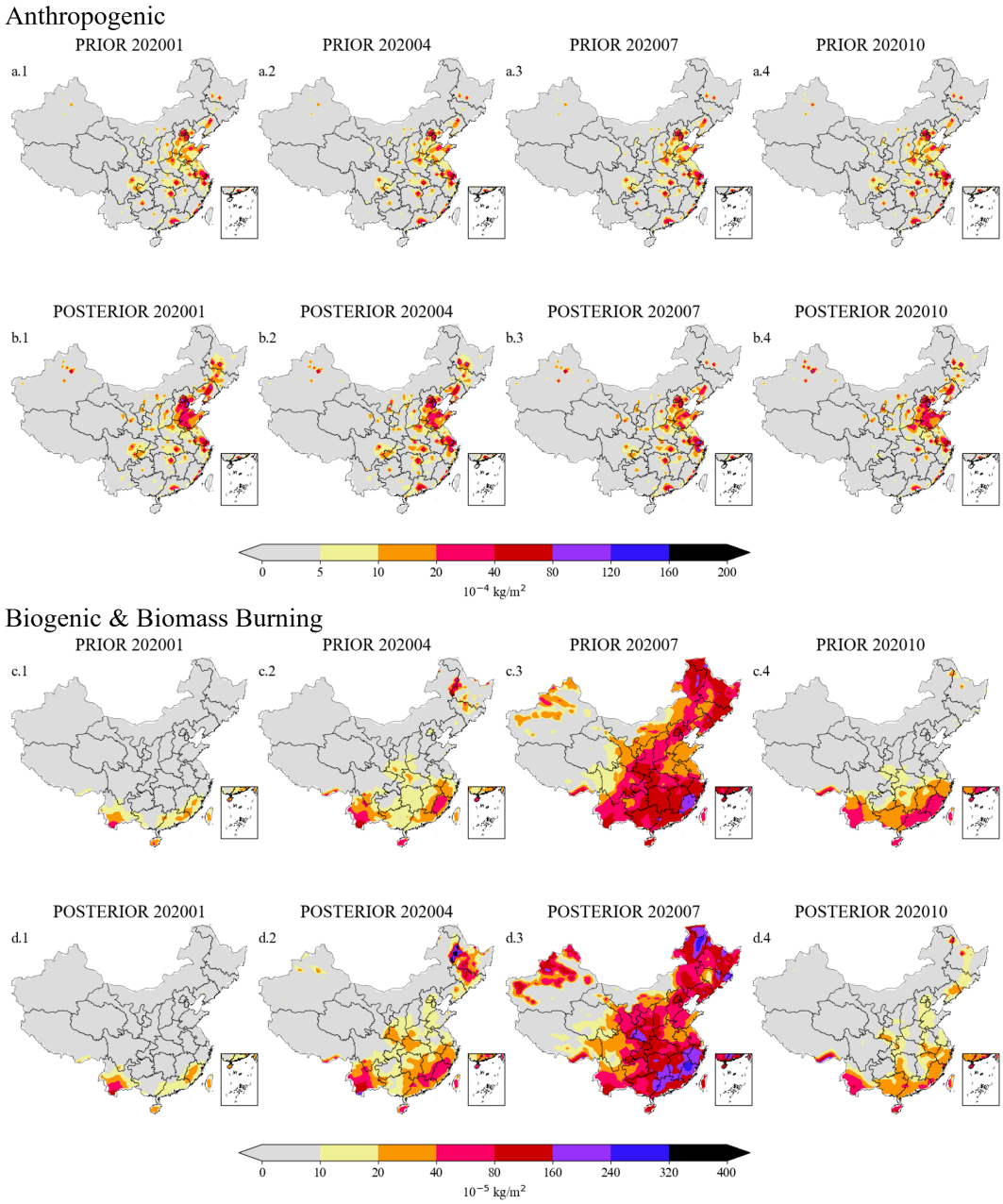

Figure S1. The results obtained by assimilating TROPOMI formaldehyde observations. The upper figures show the spatial distributions of the anthropogenic NMVOC emissions form the prior (a) and posterior (b) results in January (a.1, b.1), April (a.2, b.2), July (a.3, b.3), October (a.4, b.4). The lower figures show the spatial distributions of the biogenic and biomass burning NMVOC emission form the prior (c) and posterior (d) results in January (c.1, d.1), April (c.2, d.2), July (c.3, d.3), October (c.4, d.4).

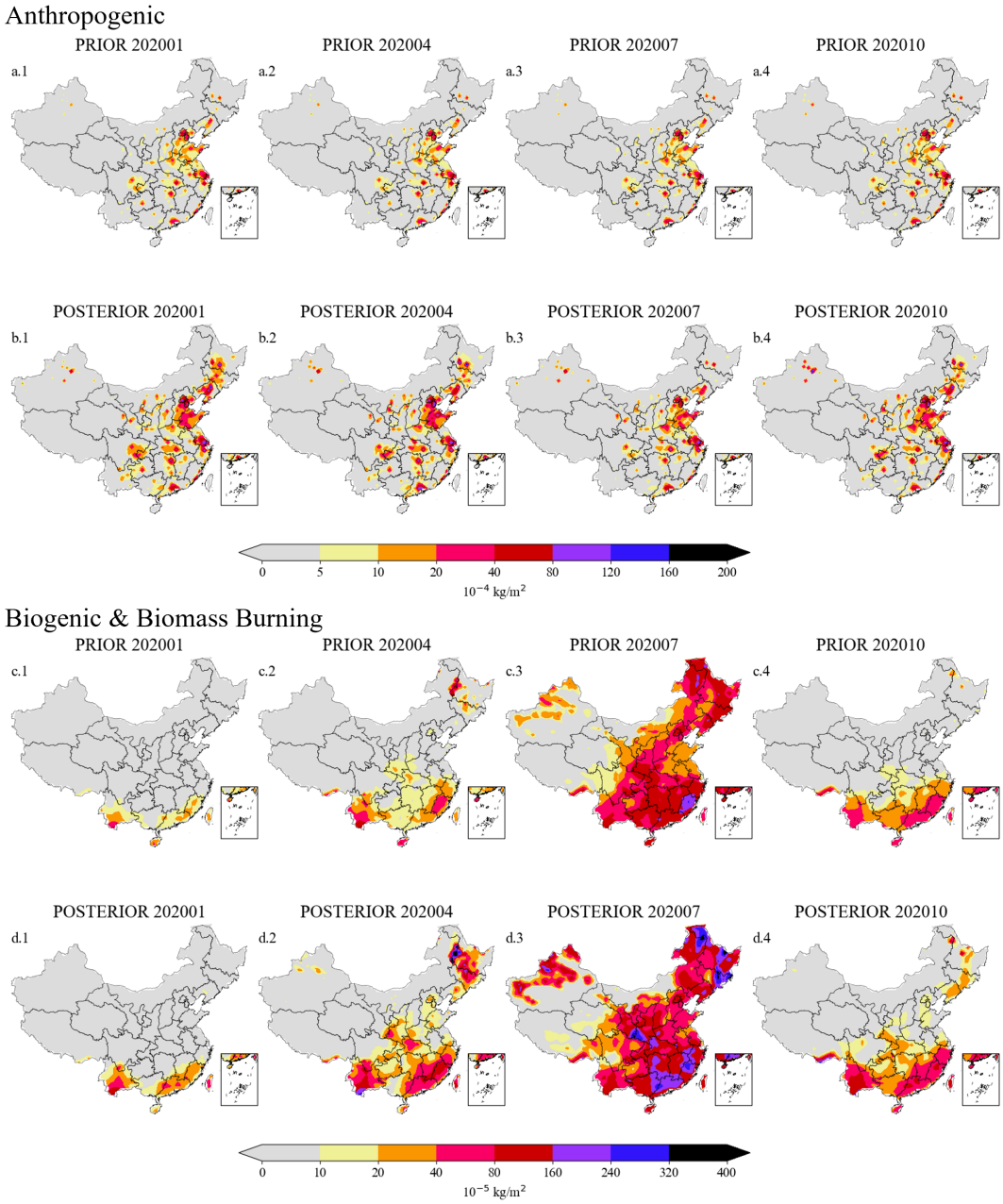

Figure S2. The results obtained by assimilating the combined data from TROPOMI and OMPS formaldehyde observations.The upper figures show the spatial distributions of the anthropogenic NMVOCs emission form the prior (a) and posterior (b) results in January (a.1, b.1), April (a.2, b.2), July (a.3, b.3), October (a.4, b.4). The lower figures show the spatial distributions of the biogenic and biomass burning NMVOC emission form the prior (c) and posterior (d) results in January (c.1, d.1), April (c.2, d.2), July (c.3, d.3), October (c.4, d.4).

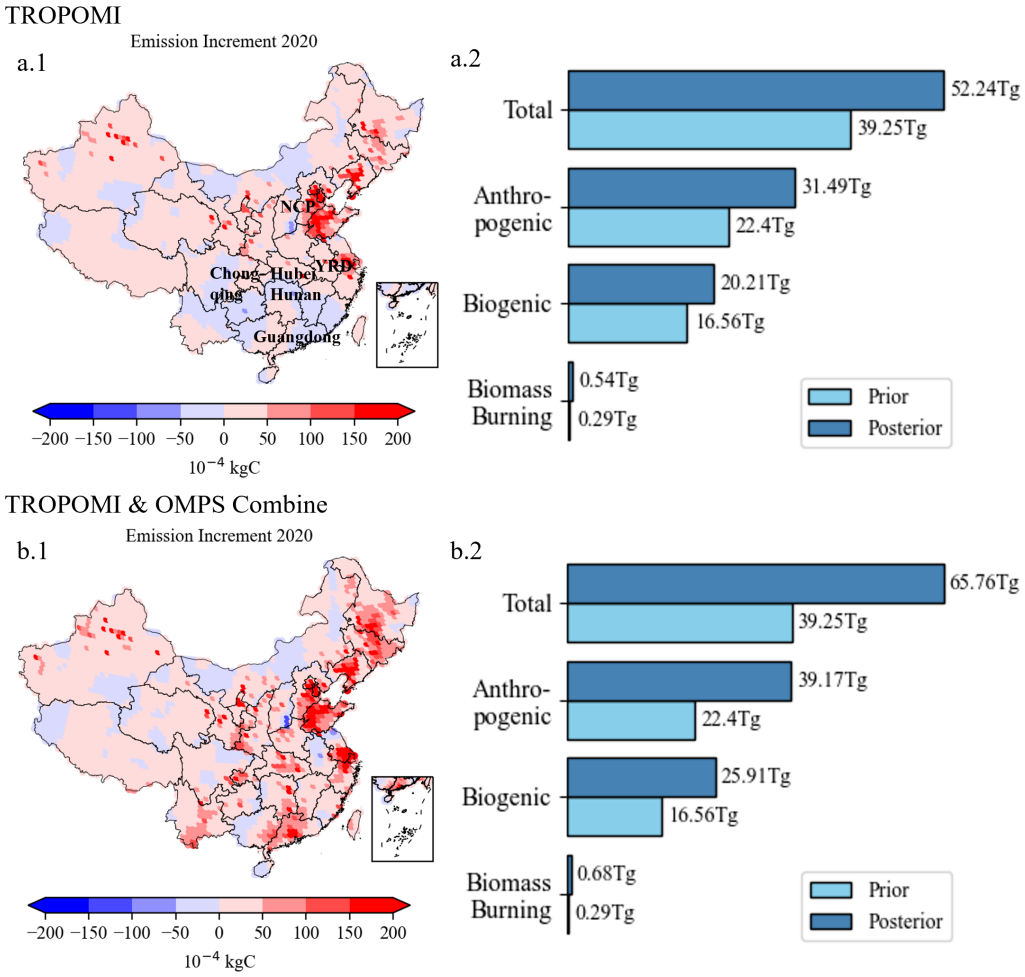

Figure S3. The increments obtained in the assimilation (a). Panel (b) compares the prior and posterior annual NMVOC emission, including total emissions, anthropogenic, biogenic, and biomass burning.